RSC Sustainability

ROYAL SOCIETY OF CHEMISTRY

PAPER

View Article Online
View Journal | View Issue

Cite this: *RSC Sustainability*, 2025, **3**, 1461

Thermo-rheological and tribological properties of low- and high-oleic vegetable oils as sustainable bio-based lubricants†

Abiodun Saka,[ab] Tobechukwu K. Abor,[c] Anthony C. Okafor[c] and Monday U. Okoronkwo *[ab]

Vegetable oil-based lubricants have attracted increased research attention in recent decades as sustainable alternatives to conventional petroleum-based lubricants in metal machining. However, more studies are required to fully elucidate the thermo-rheological and tribological properties. This study presents an investigation of the thermo-rheological and tribological properties of different vegetable oils, including low- and high-oleic soybean oil, high-oleic sunflower, safflower, and canola oils. The lubricity, and evolution of viscosity and thermodynamic properties as a function of temperature were investigated to obtain important parameters including the viscosity index, flow behavior index, flow activation energy, specific heat capacity, thermal conductivity, coefficient of friction, contact angle, and thermal-oxidative decomposition profile. The properties were compared with those obtained with mineral oil, conventional emulsion coolant (CEC), and a commercial bio-based lubricant, Acculube LB-2000, commonly used for metal cutting applications. The vegetable oils displayed comparable properties to the commercial LB-2000 lubricant and pure mineral oil, featuring Newtonian fluid characteristics, high viscosity indices, high flow activation energy, low specific heat capacity and thermal conductivity, and high thermal-oxidative stability. Generally, vegetable oils with high oleic acid content featured higher rheo-thermal stability, higher contact angle, and better performance in reducing the coefficient of friction. On the other hand, CEC displayed non-Newtonian fluid behavior with lower initial viscosity and flow activation energy, and lower thermal-oxidative stability, but comparatively higher specific heat capacity and thermal conductivity compared to the vegetable oils. Compared to pure mineral oil, the vegetable oils show higher oxidative-thermal stability, thermal conductivity and specific heat capacity, and better lubrication performance in the mixed and hydrodynamic lubrication regimes of the Stribeck curve. The results provide important datasets that will contribute to improving the database on the properties of vegetable oils to guide their utilization in designing sustainable vegetable-oil-based biodegradable lubricants.

Received 28th September 2024
Accepted 23rd January 2025

DOI: 10.1039/d4su00605d

rsc.li/rscsus

Sustainability spotlight

This study investigates the lubrication properties of vegetable oils, elucidating their potential for use as a non-toxic, renewable, sustainable, and biodegradable alternative to conventional petroleum-based lubricants. The adoption of renewable, environmentally friendly, and biodegradable lubricants derived from vegetable oils will advance the following SDG agenda goals: Good health and well-being (SDG3), Clean water and sanitation (SDG6); Sustainable cities and communities (SDG11); Responsible consumption and production (SDG12); and Climate action (SDG13).

1 Introduction

With growing concerns over environmental degradation, the need for sustainable alternatives in all areas of life has become increasingly critical. One area of focus has been the shift away from conventional mineral-based lubricants, which are known to contribute to environmental pollution and pose health risks. Among the potential alternatives, vegetable oils have garnered attention due to their biodegradability, non-toxic nature, and renewability. Early research has highlighted the promise of vegetable oils for lubricant applications, largely due to their

[a]*Sustainable Materials Laboratory (SusMatLab), Missouri University of Science and Technology, Rolla, Missouri 65409, USA. E-mail: okoronkwom@mst.edu; Tel: +1-573-341-4349*

[b]*Linda and Bipin Doshi Department of Chemical and Biochemical Engineering, Missouri University of Science and Technology, Rolla, Missouri 65409, USA*

[c]*Department of Mechanical and Aerospace Engineering, Missouri University of Science and Technology, Rolla, Missouri 65409, USA*

† Electronic supplementary information (ESI) available. See DOI: https://doi.org/10.1039/d4su00605d

unsaturated fatty acid profiles.[1–3] However, despite the rising interest in these oils, research into their thermo-rheological properties—an essential performance indicator for lubricants—remains underexplored.

The rise of advanced machining processes for difficult-to-cut materials has driven the need for high-performance lubricants. While traditional lubricants are effective, they present considerable environmental issues due to their non-biodegradable nature. Conventional Emulsion Coolant (CEC) is frequently used in industrial machining, particularly for challenging materials like Inconel 718.[4] CEC is recognized for its excellent cooling capabilities and moderate lubrication of metal alloy surfaces. However, it is often applied in large volumes to flood the cutting zone, which exposes operators to non-biodegradable hydrocarbons that pose health risks and contribute to environmental pollution. Consequently, there has been growing interest in developing biodegradable lubricants as a more sustainable and eco-friendly alternative.[3,5–7]

One major concern in the equipment lubrication industry is the leakage of non-biodegradable mineral lubricants into the environment. When a lubricant system fails, it can directly contaminate soil and water, while volatile lubricants may pollute the air.[8] As environmental awareness has increased, technological advancements in lubrication have been increasingly driven by this growing trend.[9] Due to the limitations of conventional lubricants, biodegradable alternatives have gained popularity in environmentally sensitive areas. By transitioning to bio-lubricants, advanced manufacturing businesses that rely on lubricants for machining can reduce overall tool costs, enhance product quality, and promote a safer workplace.

Biodegradable lubricants, particularly those sourced from vegetable oils, have demonstrated significant potential in advanced machining applications like minimum quantity lubrication (MQL),[10] due to their inherent lubricity, high viscosity index, and low volatility. Masripan *et al.*[5] studied the properties of soybean oil, concluding that its lower toxicity, excellent lubricating capabilities, high viscosity index, and high flash point make it an ideal alternative base oil for lubricants. Similarly, Stanciu *et al.* investigated the viscosity index of four vegetable oils used as biodegradable lubricants, finding that soybean oil had the highest viscosity index (170), while rapeseed oil had the lowest (143).[11] Equally, high oleic sunflower,[12–14] safflower,[15,16] and canola oil[17] have also been reported to exhibit favorable lubricant properties.

Despite the promising properties of vegetable oils, their widespread use as lubricants is limited by drawbacks such as low thermal conductivity, oxidative stability and high pour points.[18] However, research has shown that modifying the chemistry of vegetable oils—either through genetic alterations to adjust their fatty acid profiles or through chemical processes like hydrogenation and saponification/esterification—can improve these limitations.[19] Also, numerous studies have shown that the flow behavior, stability, and thermal conductivity properties of vegetable oils can be enhanced by the use of chemical additives[20–23] and nanoparticles.[8,18,24–26] While the effects of chemical modifications have been well studied, research on the impact of fatty acid profiles is more limited. In a 1995 study, Honary Lou demonstrated that a vegetable oil's oxidative stability improves as its oleic acid content increase.[27] Similarly, Glancey *et al.* found that high-oleic acid soybean and sunflower oils exhibited superior oxidative stability and lubricity in low-volume fluid power system pump tests when compared to low-oleic soybean oil and commercial canola-based hydraulic fluid.[28] However, the precise mechanisms behind these observations remain unclear.

There is a lack of comprehensive research on the temperature-dependent rheology, tribology, and thermodynamic properties of high-oleic and low-oleic oil-based lubricants. To address this knowledge gap and expand the understanding of vegetable oils' cooling and lubrication properties for the development of future sustainable bio-based lubricants, this study examined low- and high-oleic soybean oil, high-oleic sunflower, safflower, and canola oils. The analysis included temperature-dependent rheology, tribology, contact angle measurement, thermogravimetry, thermal conductivity, and heat capacity testing. This comprehensive approach offers deeper insights into the rheo-thermal lubricating characteristics of vegetable oils in comparison to commercially available lubricants.

2 Materials and methodology

2.1 Materials

The vegetable oils used in this study included high- and low-oleic soybean oil (sourced from ADM – Archer Daniels Midland Inc., Decatur, IL, USA, and Thermo Fisher Scientific Inc., USA, respectively), high-oleic sunflower oil, high-oleic safflower oil (both from AVO – American Vegetable Oil Inc., USA), and high oleic canola oil (from Cargill Inc., USA). These oils were selected due to their potential for industrial applications and their abundance in the USA. The oleic acid content, reflecting their monounsaturated fat levels, is presented in Table 1. Prior to the experiment, the oils were stored in airtight containers at a constant temperature of 25 °C. A commercially available bio-based heavy-duty metalworking lubricant, Accu-Lube LB-2000 (ITW, Glenview, IL, USA), served as the reference bio-based lubricant, while the conventional emulsion coolants (CEC) reference fluid was prepared using 10% Valcool VP-TECH-005B semi-synthetic oil (MSC Industrial Supply, Melville, NY, USA), blended with 90% water. Additionally, the study was benchmarked with pure petroleum-based mineral oil (specific gravity = 0.854) purchased from MilliporeSigma Milwaukee, WI, US.

2.2 FTIR spectroscopy

The FTIR analysis was performed using a Fourier-Transform Infrared Spectrometer (Thermo Scientific Nicolet iS10), equipped with Attenuated Total Reflectance (ATR) Diamond Cell. The spectrometer was operated in transmission mode with a spectral range of 4000–400 cm^{-1} and a resolution of 4 cm^{-1}. For each sample, 32 scans were collected and averaged to improve the signal-to-noise ratio. The resulting spectra were then normalized, and baseline corrected using the OMNIC software

Table 1 List of oils and lubricants studied

Fluid ID	Description	Fatty acid contents (%)			
		Mono-unsaturated (% oleic acid)	Poly-unsaturated	Saturated	Trans
HOSO	High oleic soybean oil	74.5	11.0	13.0	1.5
Safflower	High-oleic safflower oil	78.6	14.3	7.1	0
Sunflower	Sunflower	57.1	28.6	14.3	0
Canola	Canola	64.3	28.6	7.1	0
LOSO	Low-oleic soybean oil (LOSO)	24.5	58.5	16.0	1.0
LB-2000	Acculube LB-2000	—	—	—	—
CEC	10% valcool VP-TECH-005B	—	—	—	—
Mineral oil	Mineral oil	—	—	—	—

(Thermo Scientific) to facilitate comparison between different samples. The obtained FTIR spectra were analyzed to identify the characteristic absorption bands corresponding to the functional groups present in the fluids. The peak positions and intensities were compared among the different samples to determine any significant differences in their chemical compositions. The test was done thrice to ensure the reliability and reproducibility of the results.

2.3 Viscosity measurement

The viscosities of the selected biodegradable oils were evaluated using a Discovery Hybrid Rheometer (DHR2)[29,30] from TA Instruments, operated with the accompanying Trios software (Version 4.4.0.41128). This instrument is renowned for its precision and reliability in rheological measurements. Before each experiment, the rheometer underwent a calibration process. The DIN Concentric cylinder geometry equipped with a Peltier temperature control system was used. The geometry was set with a 5914 μm operating gap. The torque tolerance was set at 1%, and the controlled axial force sensitivity was adjusted to 0.1 N. The Peltier concentric cylinder is ingeniously designed to ensure precise temperature control and efficient heating. It features four Peltier heating elements in close contact with a lower cup geometry, which is secured by an insulating jacket. This arrangement facilitates rapid and effective heat transfer up the cup's wall. Additionally, a platinum resistance thermometer is positioned near the top of the cup, enabling accurate temperature measurement and control. For each experiment, 23 mL of the sample was poured into the lower cup geometry. The TA TRIOS software was programmed to capture the shear stress (Pa s) at intervals of shear rate ranges of 0–100 s^{-1}. The experiment was conducted at temperatures of 25, 35, 45, 55, 65, 70, and 80 °C.

The shear stress *versus* shear rate curves were fitted to the Newtonian, Bingham, and Herschel–Bulkley models to obtain relevant rheological parameters, vis-a-vis, viscosity and flow behavior index parameters (eqn (1)–(3))[31–35]

$$\sigma = \eta\dot{\gamma} \quad (1)$$

$$\sigma = \sigma_y + \eta\dot{\gamma} \quad (2)$$

$$\sigma = \sigma_y + k\dot{\gamma}^n \quad (3)$$

where σ is shear stress (Pa), η is viscosity (Pa s), $\dot{\gamma}$ is shear rate (s^{-1}), σ_y is yield stress (Pa), k is consistency (Pa s^n), and n is the power law index or flow behavior index.

The obtained viscosity as a function of temperature was used to determine the flow activation energy by utilizing the Arrhenius relationship (eqn (4) and (5)) as previously illustrated by Kim *et al.*[36]

$$\eta = A\exp\left(\frac{E_a}{RT}\right) \quad (4)$$

$$\ln(\eta) = \ln(A) - \frac{E_a}{RT} \quad (5)$$

where η is viscosity, E_a is the flow activation energy in J mol^{-1}, R is the gas constant (8.314 J mol^{-1} K^{-1}), and T is the temperature in Kelvin. The plot of the natural logarithm of viscosity $\ln(\eta)$ against the reciprocal of the temperature in Kelvin $(1/T)$, features a linear curve with the slope $-(E_a/R)$ from where the activation energy can then be calculated.[37] This method assumes the oil's behavior aligns with the Arrhenius equation across the temperature range and that other viscosity-influencing factors are controlled. Flow activation energy is a measure of the energy required to initiate flow in a lubricant. It represents the temperature sensitivity of the lubricant's viscosity on a molecular level.

Additionally, in accordance with the guidelines set forth by ASTM D2270, the viscosity index of each vegetable oil was determined. These viscosity measurements were conducted at temperatures of 40 and 100 degrees Celsius.[11,38]

2.4 Thermogravimetric analysis

Thermogravimetric analysis (TGA) and its derivative (DTG) are techniques used to investigate the thermal behavior of materials.[39] These techniques are particularly useful for understanding the thermal stability, decomposition, and compositional changes of organic materials like vegetable oils.[40] STA 449 Jupiter NETZSCH instrument was used to analyze the thermogravimetric properties of the fluids under investigation. The STA 449 instrument is a simultaneous thermal analyzer that allows the measurement of mass changes and thermal

effects in a wide temperature range of −150 °C to 2400 °C. The materials and equipment used for this analysis included high-purity air gas cylinders, a sample of biodegradable oil, a ceramic crucible, and an analytical balance. The STA 449 Jupiter NETZSCH machine is controlled by the Proteus® software.

The sample preparation involved measuring approximately 10–20 mg of the biodegradable oil sample using an analytical balance and placing it in a ceramic crucible. This sample size is typically used in TGA to ensure a robust signal-to-noise ratio and precise measurements while preventing sample overflow during the analysis. Prior to the analysis, the instrument was calibrated according to the manufacturer's instructions to ensure the accuracy of the measurements. A baseline test was conducted with an empty crucible under identical conditions to the sample run, including the temperature range, heating rate, and airflow rate. This baseline test helps to correct any changes in mass due to the buoyancy effect or the weight loss of the crucible. The crucible containing the sample was then placed in the TGA instrument, and the system was purged with high-purity air to remove any residual gases. The use of air provides a source of oxygen, which is crucial for understanding the oxidation behavior of the fluid. The heating process was initiated at a temperature of 25 °C and increased at a rate of 10 °C per minute up to 600 °C, with a constant airflow rate of 20 mL min^{-1} maintained throughout the experiment.

The instrument recorded the change in mass of the sample as a function of temperature, which provided a detailed profile of the thermal degradation behavior of the biodegradable oils and fluids.

2.5 Specific heat capacity

The specific heat capacity is an important thermal property of oils that indicates how much heat energy is required to raise the temperature of the oil by 1°. The specific heat capacity of the selected fluids was determined using a THT Micro Reaction Calorimeter. The materials and equipment used for this analysis included a sample of each fluid, an analytical balance, and the test sample glass vial with an 11 mm crimp cap made of PTFE. The sample preparation involved measuring a suitable amount of the fluid into the sample vial using an analytical balance and placing it in the calorimeter. Prior to the analysis, the micro reaction calorimeter was calibrated according to the manufacturer's instructions to ensure the accuracy of the measurements. A baseline test was conducted with an empty sample vial under identical conditions to the sample run, including the temperature range and temperature step (25 °C, 40 °C, 60 °C, 80 °C, 100 °C, 120 °C). The baseline test helps to correct any changes in heat capacity due to the vial or the instrument itself.

Once the test sample vial was placed in the calorimeter the heating program was set to initiate at a temperature of 24.5 °C and increase in steps of 1 °C up to 25.5 °C, then decrease back to 24.5 °C. This process was repeated for other temperature points (39.5 °C to 40.5 °C, 59.5 °C to 60.5 °C, and up to 119.5 °C to 120.5 °C). The median value of each temperature range is the temperature at which the specific heat capacity was measured.

The calorimeter monitored the heat flow as a function of temperature, automatically recording the heat flow at each temperature point. After the experiment, the data was analyzed to determine the specific heat capacity of the biodegradable oil at each temperature point. The results were compared with the baseline to correct for any instrumental effects.

2.6 Thermal conductivity

The thermal conductivity of the fluids was determined using the Thermtest TLS-100 portable thermal conductivity meter. The sensor probe, which is immersed in the fluid under investigation, operates on the transient line source (TLS) method. This probe features a thin wire that serves dual purposes: it acts as a heat source and a temperature sensor. When a known quantity of electrical energy is supplied, the wire heats up, causing a temperature increase in the surrounding material.

The sensor probe was inserted into a sample container, which was then placed in an ISOTEMP 210 Fischer Scientific water bath. To ensure the accuracy of the measurements, the sensor probe was calibrated before the commencement of the experiment. The water bath was conditioned to a temperature of 21 °C (room temperature). Once the probe was immersed in the fluid at a specific temperature, it was allowed to equalize for 15 to 20 minutes to mitigate temperature drift.

Upon initiation of the test, the main unit was activated, and the system monitored the temperature increase over a specified duration of 120 seconds. The rate of this temperature increase is directly proportional to the fluid's thermal conductivity, which was subsequently calculated according to Fourier's law, following eqn (6). Each measurement was repeated three times, and the reading with the lowest percentage error was selected. In cases where all three measurements had a percentage error of less than 0.001, the average of the three measurements was taken.

$$k = \frac{q}{4\pi a} \tag{6}$$

where, k = thermal conductivity (W m^{-1} K^{-1}); q = heating power (W m^{-1}); a = slope of the temperature rise over the logarithm of time.

2.7 Tribology

Tribology enables the measurement of the lubricating effects performance of each fluid. The TA Instrument's Tribo-rheometry Accessory integrated with the Discovery HR-2 rheometer was used for tribology studies.[41,42] The three-ball-on-plate geometry, consisting of stainless-steel hemispheres, each with a diameter of $\frac{1}{4}$ inch, was utilized for this study. A disposable 40 mm aluminum plate was used as the bottom plate. The TA Instruments tribology set-up was designed following the concepts of ball-on-disc in ASTM G99 Standard,[43] commonly used for lubricant tests.[41,44,45] The schematics of the tribo-rheology geometry used is shown in Fig. 1.

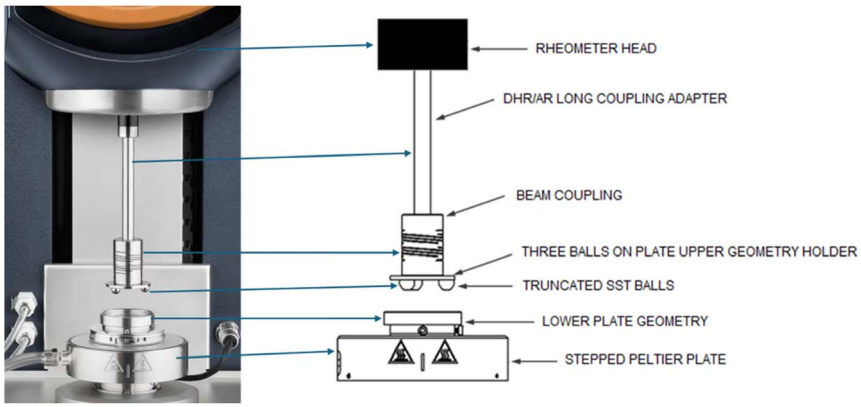

Fig. 1 Schematics of the tribo-rheological setup utilized in the study, in accordance with the instruction manual provided by TA Instruments-Waters LLC.[42]

For the test, a 1.5 mL fluid sample was carefully measured and transferred onto the lower aluminum plate and allowed to equilibrate to 25 °C for 30 seconds. The upper geometry with the three balls was lowered to contact the bottom plate and the normal force of 6 N was applied while a sweep test varying the sliding speed from 0 to 250 rad s^{-1} was conducted. The angular velocity range was chosen to provide a comprehensive characterization of the tribological behavior that covers the full range of the Stribeck curve regimes. With the aid of the TA TRIOS Software, the torque values at each velocity were recorded as well as the friction coefficient (μ) calculated using eqn (7):

$$\mu = M/(d \times F_N) \quad (7)$$

where M represents the torque (N m), d is the arm length fixed at 0.015 m, and F_N is the normal force (N). The average friction coefficient values were determined from triplicate measurements. The obtained data were analyzed by calculating Hersey's number which is a function of the sliding speed, viscosity, and the normal force exerted, and the results were interpreted in terms of the tribological performance of the samples in different lubrication regimes of the Stribeck curve.[46]

2.8 Contact angle measurement

The contact angle of the lubricants on a glass plate was measured using the L2004A1 Ossila Contact Angle Goniometer (Ossila BV, Netherlands). The goniometer was equipped with a camera and PC software that provided a simple and intuitive interface for contact angle measurements. A disposable glass plate was used as the substrate for the contact angle measurements. The glass plate was thoroughly cleaned to remove any contaminants or residues that could affect the wetting behavior of the lubricant. The cleaned glass plate was then placed in the center of the vertical tilt stage of the goniometer. A microlitre syringe was used to dispense a small droplet (approximately 5–10 μL) of the lubricant onto the glass plate. The stage height was adjusted until the droplet was visible in the camera's field of view. The camera lens was focused to ensure a sharp image of the droplet on the software display.

The Ossila Contact Angle software was used to record a video of the droplet spreading on the glass plate. The recording duration was set to an appropriate length (*e.g.*, 30 seconds) to capture the initial spreading behavior and the equilibrium contact angle. The frame rate was set to 20 frames per second to provide sufficient temporal resolution. After recording the video, the software's analysis tools were used to measure the contact angle. The region of interest (ROI) was adjusted to enclose the droplet, with the baseline aligned with the glass plate surface. The software detected the edges of the droplet within the ROI and applied a polynomial fitting to determine the contact angle. The average of the left and right contact angles was recorded for each frame of the video. The measurements were repeated for multiple droplets (at least 3) to ensure reproducibility and statistical significance. Using a disposable glass plate as the substrate for contact angle measurements offered several advantages. First, glass plates provide a uniform and consistent surface, allowing for better comparability between different lubricant samples. Second, glass plates can be easily cleaned and sterilized, minimizing the risk of contamination. Third, the transparency of the glass allows for clear visualization and imaging of the droplet, which is essential for accurate measurements. Finally, using disposable plates eliminates the need for extensive cleaning between measurements, saving time and effort. While it is acknowledged that the actual material to be lubricated may provide more relevant information about the lubricant's wetting behavior in real-world applications, using glass plates as a standardized substrate is common in contact angle studies. The results obtained on glass can serve as a baseline for comparing the wetting properties of different lubricants and guide the selection of promising candidates for further testing on the actual material surfaces like steel or Inconel.

3 Results and discussion

3.1 FTIR spectra of the fluids

The chemistry of the fluids was analyzed using FTIR. Fig. 2a shows the IR spectra of the Conventional Emulsion Coolant

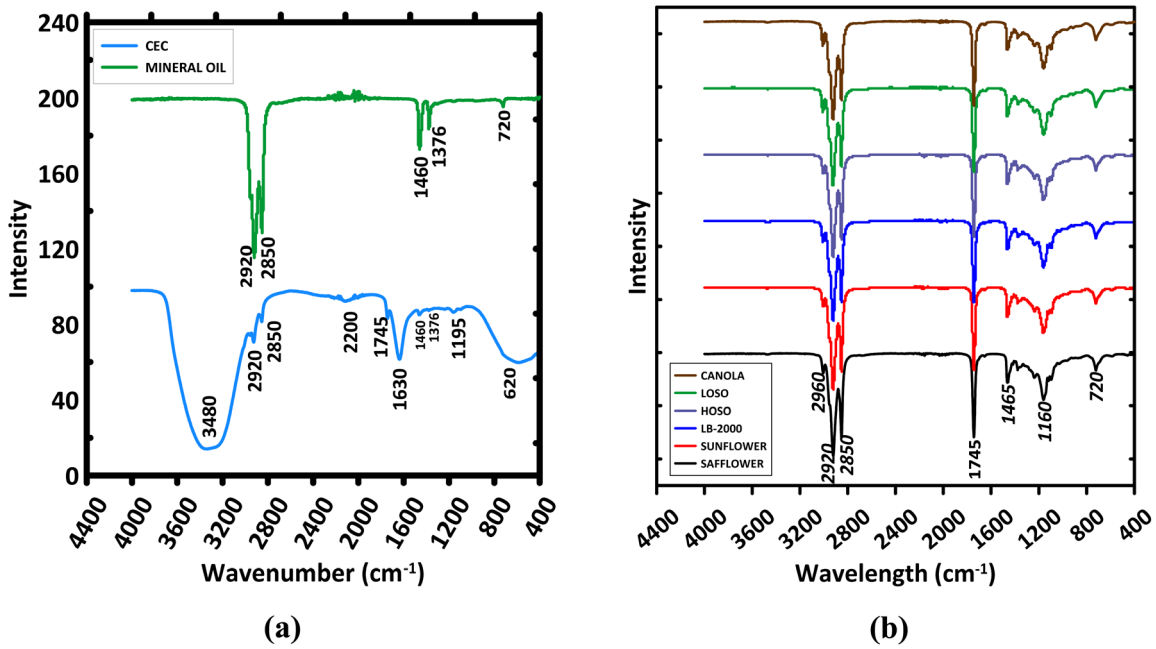

Fig. 2 FTIR spectra of (a) conventional emulsion coolant and mineral oil, (b) the vegetable oils and LB-2000.

(CEC) and mineral oil. The CEC exhibits a broad absorption band between 3200–3600 cm^{-1}, often linked to alcohols, phenols, or water due to O–H stretching and hydrogen bonding.[47,48] These bands are mostly due to water, as CEC contains 90% water. Similarly, the band around 1620 cm^{-1} is attributed to H–O–H bending in water.[49,50] The minor absorption band at ~2200 cm^{-1} in the CEC is attributed to potential nitrile additive in CEC,[51–53] the absorption band at ~1745 cm^{-1} and 1195 cm^{-1} are attributed to carbonyl C=O and C–O stretch of aliphatic esters, respectively,[54] while minor hydrocarbon absorption bands, CH_2 (2920 cm^{-1} and 1460 cm^{-1}) and CH_3 (2850 cm^{-1} and 1376 cm^{-1}), are due to the mineral oil component which agrees with the spectra of the pure mineral oil in Fig. 2a.[55–57] The band at 720 cm^{-1} in the mineral oil is attributed to C–H group[55,57] and the broadened absorption band around 620 cm^{-1} in the CEC spectra is due to hindered water rotation.[58]

In contrast, Fig. 2b shows that all vegetable oils and LB-2000 exhibit negligible absorption between 3200–3600 cm^{-1} but have strong absorption bands between 2800–3000 cm^{-1}, corresponding to C–H stretching in long-chain fatty acids. CH_2 vibrations appear at 2850 cm^{-1} (symmetric) and 2920 cm^{-1} (asymmetric), while CH_3 groups stretch at 2870 cm^{-1} (symmetric) and 2960 cm^{-1} (asymmetric).[59,60] This confirms the presence of long-chain hydrocarbons in all oils and LB-2000.

A strong band around 1740–1750 cm^{-1}, signifying C=O stretching in ester carbonyl groups, is present in all vegetable oils, marking their triglyceride content.[61] The weak band around 1650–1660 cm^{-1} reflects C=C stretching in unsaturated fatty acids, varying among oils, with slightly higher peaks in safflower, sunflower, and HOSO due to their higher unsaturation.[59,60]

Bands between 1350–1500 cm^{-1} relate to CH_2 and CH_3 bending, present in all oils, while those from 1000–1300 cm^{-1}, centered at ~1160 cm^{-1}, indicate C–O stretching in ester bonds, underscoring the triglyceride structure.[61] The region of 650–1000 cm^{-1} shows a band around 720 cm^{-1}, indicating =C–H bending.[59,60]

Collectively, the FTIR spectra of the vegetable oil samples demonstrated a remarkable degree of similarity with the LB-2000, particularly in the identification of common functional groups characteristic of vegetable oils. Nonetheless, nuanced variations in the peak intensities and positions indicated differential concentrations of specific molecular entities or the presence of unique compounds within individual samples.

The FTIR spectra of CEC and vegetable oils reveal significant differences in their chemical compositions. The presence of a broad O–H stretching band in CEC confirms water content, while vegetable oils show characteristic peaks for long-chain fatty acids and triglycerides. The differences in the intensity and presence of specific absorption bands highlight the unique molecular structures of CEC and vegetable oils.

3.2 Thermo-rheological behavior

3.2.1 Flow behavior. Fig. 3a and b show the representative flow curves of the vegetable oils, and flow curves of the mineral oil as a function of temperature, wherein both systems displayed Newtonian fluid characteristics with the shear stress *vs.* shear rate curves exhibiting straight lines that pass through the origin.[62] As the temperatures increase, the slope of the curves decreases but the Newtonian properties are maintained. Hence the oils were fitted to the Newtonian model shown in eqn (1), to obtain the viscosity discussed in Section 3.3. Similarly, Fig. 3c shows the flow curves for the CEC which exhibit non-Newtonian

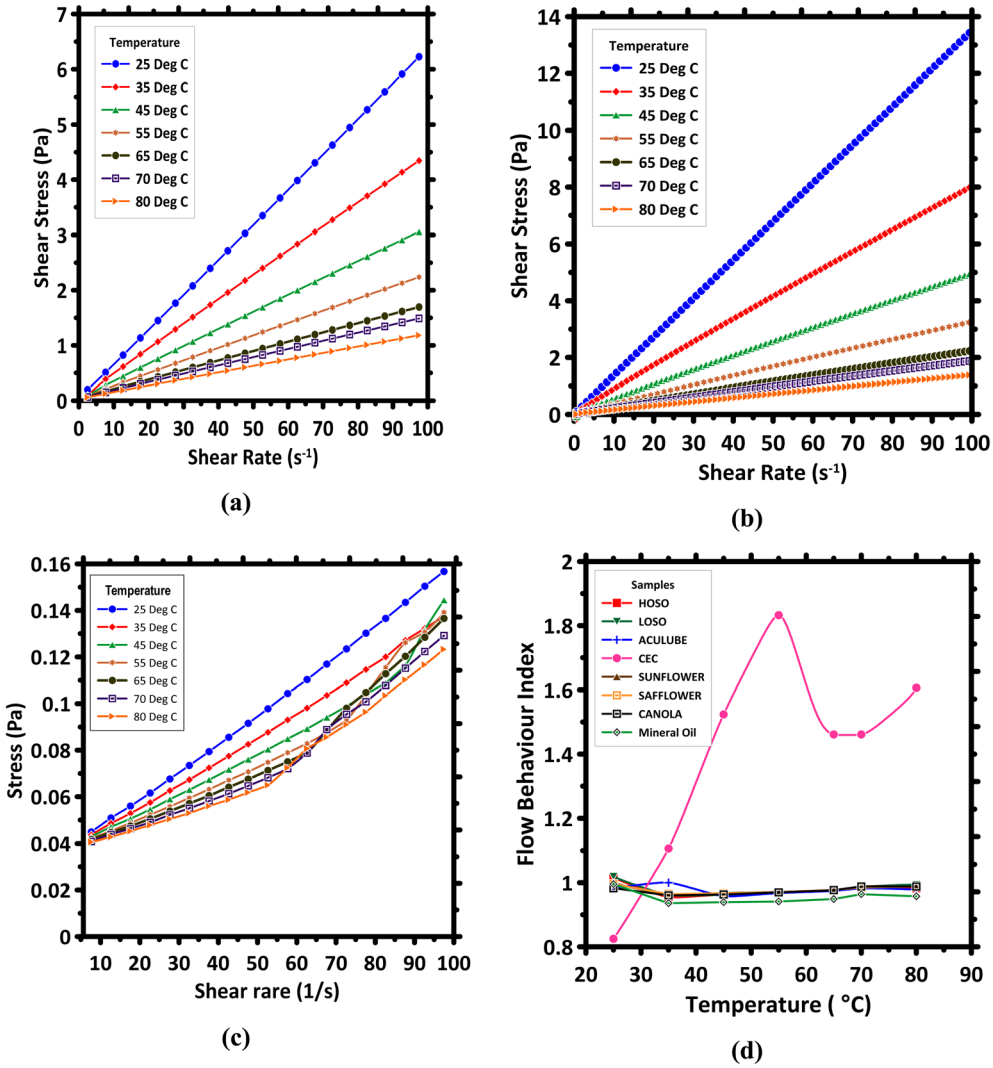

Fig. 3 Temperature-dependent flow behavior of the fluids: (a) flow curves of HOSO as a function of temperature, as a representative of the vegetable oils; (b) flow curve of the mineral oil as a function of temperature; (c) flow curve of CEC as a function of temperature; (d) flow behavior index of CEC compared to the vegetable oils, mineral oil, and LB-2000.

yield stress or Bingham fluid characteristics[31–34] and were therefore fitted to the Bingham model in eqn (2), to obtain the viscosity. However, it was observed that as the temperature increased, the CEC displayed a shear-thickening behavior seen in the upward curvature of the flow curve (Fig. 3c). Hence the curves were also fitted to Herschel Buckley's modified Bingham model (eqn (3)), to estimate the flow behavior index which is shown in Fig. 3d.

As shown in Fig. 3d, as the temperature increased from 25 °C to 80 °C, the flow behavior index remained relatively constant at ~1.0 for the vegetable oils, mineral oil, and LB-2000 but increased for the CEC, supporting the Newtonian behavior of the vegetable oils, mineral oil, and LB-2000, and non-Newtonian shear-thickening behavior of the CEC as a function of temperature.[31–34] The flow behavior index trend of CEC showed a drop after 55 °C which can be attributed to an onset of gradual destabilization of the emulsion or phase inversion phenomenon where the continuous and dispersed phase switch roles. It is known that high temperatures can disrupt the thermodynamic stability emulsions, instigating phase separation and reducing the homogeneity of the system.[63] A change in the CEC original color was also observed at this temperature (55 °C), physically confirming the phase inversion phenomenon. Yet, at 80 °C, a reversal of droplet coalescence may occur due to the heightened molecular motion and decreased viscosity of the oil phase.

3.2.2 Flow activation energy. From the experimental data, as shown in Fig. 4a, an inverse correlation between temperature and viscosity of vegetable oils was observed. Elevated temperatures induce an increase in both molecular velocity and kinetic energy, which in turn reduces viscosity. This behavior is in line with several studies by researchers who also affirmed the pronounced influence of temperature on the viscosity of vegetable oils.[64,65] The viscosity of a fluid affects the fluid's ability to form a film between moving parts and its effectiveness in reducing friction and wear. Thus, maintaining sufficient

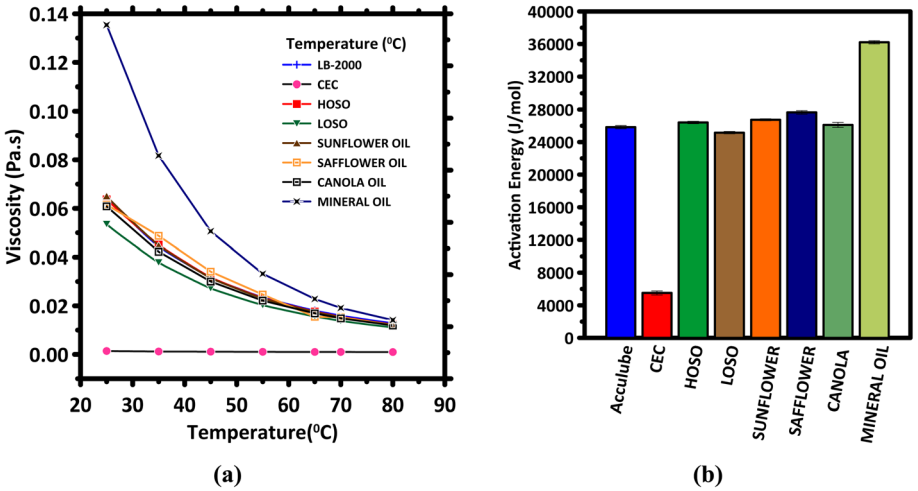

Fig. 4 (a) A graph showing the viscosity–temperature relationship of different vegetable oils compared to CEC, (b): a bar graph comparing the activation energy of various vegetable oils to that of CEC.

viscosity at the operating temperature range is important. If the viscosity is too low, the fluid film may break down and fail to protect the moving parts, leading to increased wear and potential failure. It was observed that the viscosity of CEC is significantly low at all tested temperatures compared to the vegetable oils and investigated LB-2000. However, mineral oil displayed the highest viscosity (Fig. 4a). This indicates that the CEC may not have the ability to form sufficient thin films to protect the cutting zone/moving parts and hence will feature the lowest lubrication efficiency.

According to the concept of flow activation energy,[66–69] a lubricant with higher flow activation energy means that its molecules need more energy to move past each other, resulting in higher viscosity and greater resistance to flow. These lubricants are generally more stable and better at maintaining their viscosity across a broad temperature range, as the higher energy barrier makes it harder for the molecules to move even at elevated temperatures. In contrast, lubricants with lower activation energy are more sensitive to temperature changes. As the temperature rises, their molecules gain enough energy to surpass the lower barrier, leading to a more significant reduction in viscosity.

Fig. 4b presents the flow activation energies of the fluids, showing that CEC has significantly lower activation energy (5518.50 J mol^{-1}), than the vegetable oils and LB-2000, while the pure mineral oil displayed the highest value. The low activation energy of CEC corresponds to the low viscosity values observed for CEC across the temperature range (0.000467023 Pa s at 25 °C to 0.000059792 Pa s at 80 °C). The minimal energy required for CEC to flow aligns with its role as a coolant, ensuring efficient heat transfer. However, this also makes CEC less effective as a lubricant, especially under high-load or high-temperature conditions where thicker films are needed to prevent wear during advanced machining.

All the vegetable oils show higher flow activation energies than CEC, suggesting that they are more resistant to viscosity changes with temperature, providing better stability across wider temperature ranges. However, the mineral oil's flow activation energy surpasses all the vegetable oils. As shown in Fig. 4a, the viscosity of vegetable oils and LB-2000 remains consistently higher than that of the CEC at all temperatures, even though the viscosity of the oils appears to decrease as the temperature increases. Among the vegetable oils, safflower oil has the highest activation energy, followed by sunflower oil, HOSO, canola oil, LB-2000, and LOSO. The LB-2000, a commercial vegetable-based lubricant, exhibits slightly lower activation energy than pure high oleic vegetable oils (except LOSO) but still higher than CEC, indicating a balance between improved flow and temperature stability. The difference in activation energies between high-oleic and low-oleic Soybean oils (HOSO and LOSO) suggests that the high-oleic variety may have a marginally better resistance to viscosity changes with temperature. This finding aligns with Fasina *et al.*'s explanation that the viscosities of vegetable oil samples are strongly correlated with the concentrations of monounsaturated or polyunsaturated fatty acids.[70]

3.2.3 Viscosity index. Viscosity Index (VI) is a common metric for assessing the temperature-dependent flow properties of oils and lubricants.[11,71,72] It indicates how much fluid's viscosity changes over a given temperature range. A high VI denotes superior viscosity stability across different temperatures, which is beneficial for lubrication purposes. Lubricants with high VI values resist significant thickening at low temperatures, enabling quick engine starts and efficient oil flow. Additionally, they prevent excessive thinning at high temperatures, ensuring strong lubrication and reducing oil consumption.[73]

The viscosity index is calculated based on the ASTM D2270 standard following eqn (8) and (9).

$$\mathrm{VI} = \left[\frac{(\text{anti log } N) - 1}{0.00715}\right] + 100 \quad (8)$$

$$N = \frac{\log H - \log U}{\log Y} \quad (9)$$

Y is the kinematic viscosity at 100 °C of the sample lubricant whose viscosity index is being calculated; H is the kinematic viscosity at 40 °C of an oil with a viscosity index of 100 that has the same kinematic viscosity at 100 °C as the sample lubricant, and U is the kinematic viscosity at 40 °C of the oil whose viscosity index is to be calculated. All values are in $mm^2\ s^{-1}$. The corresponding L and H values obtained with data from ASTM D2270 through interpolation are presented in Table 2.

Based on the experimental results as shown in Table 2, the high oleic oils exhibited high viscosity indices slightly above that of LB-2000, with sunflower and safflower oil exhibiting the highest viscosity index of 227.90 and 226.50, indicating their excellent ability to maintain viscosity stability over a wide temperature range. This property makes the high oleic oils an attractive choice for applications where consistent lubrication performance is required despite temperature fluctuations. On the other hand, the low oleic soybean oil displayed the lowest viscosity index 179.55, suggesting the significance of fatty acid composition in controlling the oils' resistance to viscosity changes with temperature. Nonetheless, the mineral oil exhibited the lowest viscosity index compared to the vegetable oils, consistent with the literature.[74]

The slightly lower VI values of canola oil and LB-2000 compared to the other vegetable oils may be due to differences in their chemical composition and the presence of additives in the case of LB-2000.[75,76] LOSO has the lowest viscosity index among the tested samples at 179.55. Although this value is lower than the other oils, it still represents reasonable viscosity–temperature performance. The lower VI of LOSO can be attributed to its lower oleic acid content compared to the other vegetable oils. For Conventional Emulsion Coolant (CEC), the viscosity index could not be determined due to its low kinematic viscosity, which falls below the 2 $mm^2\ s^{-1}$ threshold stipulated by the ASTM D-2270 standard.[38] This is primarily attributable to CEC's role as a coolant, for which viscosity stability over a broad temperature spectrum is often not a focal concern. Additionally, the presence of water in the emulsion contributes significantly to its low viscosity, thus invalidating its candidacy for VI measurement under the ASTM D-2270 guidelines. Kinematic viscosity, defined as the ratio of absolute viscosity (in cP) to density (in $g\ cm^{-3}$), serves as the basis for VI determination. As per ASTM D-2270, the fluid under investigation must exhibit a kinematic viscosity greater than 2 $mm^2\ s^{-1}$ and less than 70 $mm^2\ s^{-1}$ at 100 °C. These conditions ensure that the calculated VI falls within the range for which the ASTM tables are validated, typically between 2 cSt and 70 cSt.

3.3 Thermogravimetry

To assess oxidative thermal stability, thermogravimetric analysis (TGA) was conducted on the fluids in the presence of air. The results, displayed in Fig. 5a–c, indicate that all vegetable oils and LB-2000 demonstrate similar high thermal stability up to approximately 250 °C (Fig. 5a), making them suitable for high-temperature lubricant applications. The mineral oil began to degrade at a similar temperature as the vegetable oils but exhibited much more rapid degradation than the vegetable oils as depicted by its steep TGA profile (Fig. 5a). In contrast, the CEC shows the lowest oxidative thermal stability, with rapid degradation beginning around 100 °C (Fig. 5c), likely due to the high water content in the emulsion.

For the vegetable oils and LB-2000, the mass loss remains negligible up to ~250 °C. However, as the temperature exceeds 250 °C, the uniformity in TGA profiles begins to diverge, revealing unique features due to minor differences in chemical composition. The derivative thermogravimetric (DTG) profiles, depicted in Fig. 5b, highlight differences between low oleic and high oleic soybean oils. According to Fig. 5b, the first significant mass loss of low oleic soybean oil (LOSO) occurs at around 405 °C, while for high oleic soybean oil (HOSO), it is slightly higher at 430 °C. This supports the conclusion that high oleic oils possess slightly greater oxidative thermal stability, in agreement with previous studies.[77–79] In summary, the vegetable oils show comparable performance with the commercial LB-2000 displaying high thermal stability, while CEC displays low thermal stability indicating CEC's suitability is limited to low-temperature applications.

3.4 Specific heat capacity and thermal conductivity

The specific heat capacity quantifies the energy needed to raise the temperature of a unit mass of the fluid by 1 °C, which represents a critical parameter indicating a lubricant's heat-

Table 2 Viscosity index of the vegetable oils

Sample name	Viscosity@40 °C (cP)	Viscosity@100 °C (cP)	Density ($g\ cm^{-3}$)	Kinematic viscosity (U) ($mm^2\ s^{-1}$)@40 °C	Kinematic viscosity ($mm^2\ s^{-1}$)@100 °C (Y)	H	N	Viscosity index	*V–T* coefficient
LB-2000	37.42	8.22	0.9124	41.02	9.02	71.3	0.2514	209.77	0.780
Sunflower	37.70	8.74	0.8933	42.21	9.78	80.27	0.2818	227.90	0.768
HOSO	38.83	8.88	0.9307	41.72	9.54	77.37	0.2738	223.00	0.771
LOSO	29.06	6.21	0.920	31.59	6.75	45.87	0.195	179.55	0.786
Safflower	34.16	8.22	0.9392	37.16	8.75	68.18	0.2799	226.546	0.765
Canola	35.89	8.118	0.9535	37.638	8.51	65.48	0.2585	213.89	0.774
Mineral oil[a]	64.69	8.51	0.8010	80.76	10.635	90.61	0.048	116.59	0.868

[a] To estimate the uncertainty on the viscosity index, a triplicate determination was performed for the mineral oil and the standard deviation was ± 0.7487.

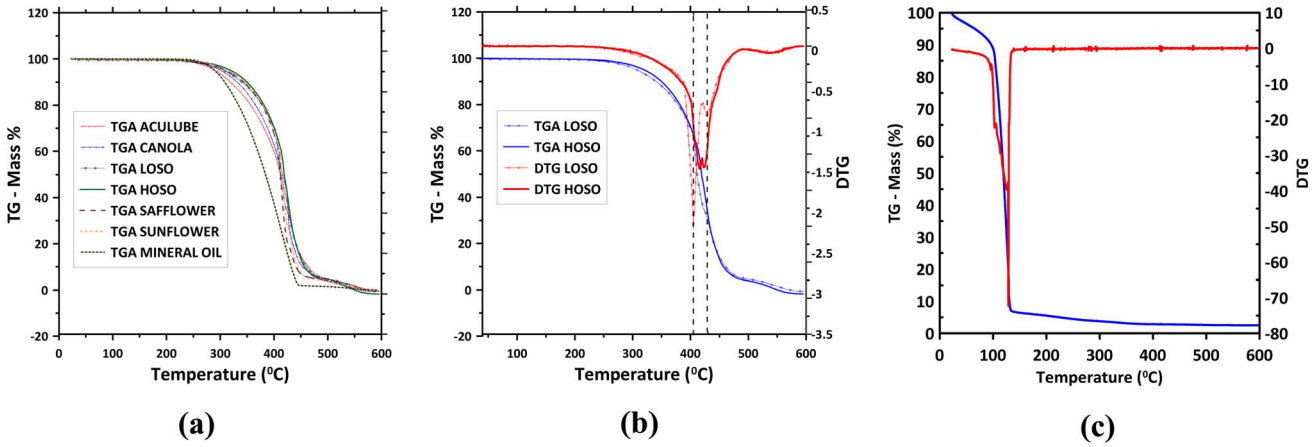

Fig. 5 (a) TGA graphs of various vegetable oils, mineral oil, and LB-2000, (b) combined TGA/DTG graphs of the low oleic and high oleic soybean oils, and (c) TGA and DTG graphs of CEC.

absorbing characteristics. On the other hand, thermal conductivity measures the ability of the fluid to conduct heat. Combined, these two parameters can reveal the cooling properties of a lubricant. A higher specific heat capacity implies that the oil can absorb more heat before experiencing a significant temperature increase, a feature especially advantageous in thermally demanding environments such as mechanical engines and intricate industrial systems.[80] Also, a high thermal conductivity ensures efficient and rapid conduction of heat away from the lubricated surface,[81] thereby helping to avoid overheating due to the friction between two surfaces during the machining of difficult-to-cut materials.[24] These properties directly influence the ability of the lubricant to dissipate heat and maintain optimal operating temperatures, which is essential for prolonging tool life and ensuring the quality of machined components.

Fig. 6a shows the specific heat capacities of the various fluids (HOSO, LOSO, LB-2000, safflower, sunflower, canola, mineral oil, and a convection emulsion coolant (CEC)), across a temperature range from 25 °C to 120 °C. The results show that CEC consistently exhibits the highest specific heat capacity across all temperatures, starting from 3.51 J per g per °C at 25 °C to 4.13 J per g per °C at 120 °C. This high specific heat capacity suggests that CEC has a superior ability to absorb and retain heat compared to vegetable oils and LB-2000, making it an effective coolant. However, the pure mineral oil shows lower heat capacity than the vegetable oils and LB-2000. Furthermore, Fig. 6b shows that CEC has significantly higher thermal conductivity compared to vegetable oils and LB-2000, wherein mineral oil again shows the lowest thermal conductivity. Fluid's ability to absorb heat fast and conduct it away from the surface reduces the risk of overheating.

The increment of specific heat capacity with temperature indicates that CEC remains effective over a wide temperature range (Fig. 6a), making it suitable for applications where rapid cooling is required. A similar increment is also seen for the vegetable oils and LB-2000 with an increase in temperature. However, the vegetable oils display relatively low specific heat

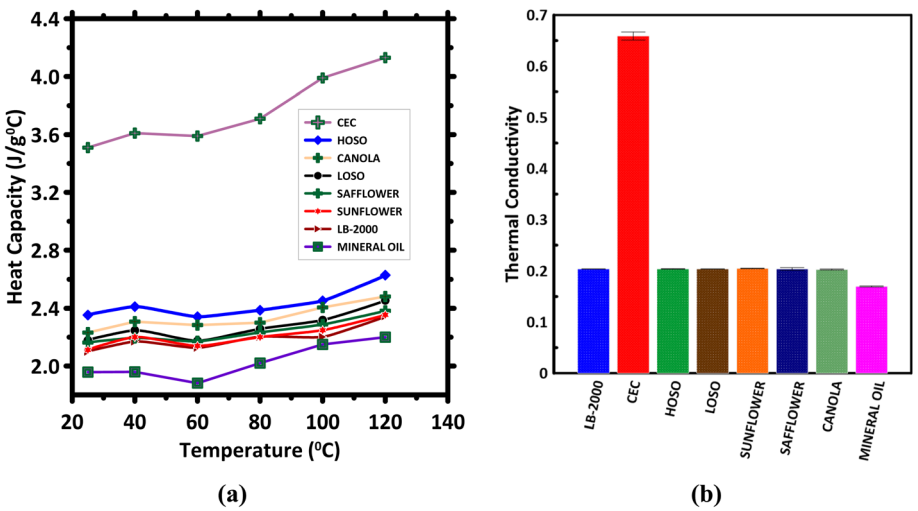

Fig. 6 Graph of: (a) specific heat capacity, and (b) thermal conductivity of the vegetable oils compared with mineral oil, LB-2000 and CEC.

capacities, generally ranging from about 2.10 to 2.45 J per g per °C, wherein the LB-2000, sunflower, and safflower oils have specific heat capacities close to each other, while HOSO, canola, and LOSO are slightly higher. Comparing soybean oils, HOSO displayed higher specific heat capacity than LOSO, suggesting high oleic acid content favors heat dissipating properties, which also agrees with high-temperature treatment studies.[79]

Overall, CEC shows superior cooling capabilities, however, vegetable oils offer the advantage of being environmentally friendly, biodegradable, and possess good rheological properties, and tribological properties (shown in subsequent section) which are crucial in applications where environmental regulations and sustainability are prioritized. To improve the cooling capacity of vegetable oil, physical or chemical modification can be employed.[8,18,24,25,80]

3.5 Lubricity and wettability

To investigate the lubricity or effectiveness of the fluids in reducing friction between two surfaces, a tribology study was conducted as described in Section 2.7. Also, the wettability properties of the fluids were examined by contact angle measurement as described in Section 2.8. Fig. 7a presents the Stribeck curve showing the coefficient of friction (COF) characteristics for the fluids as a function of Hersey number, where Hersey number is a dimensionless value calculated by multiplying velocity (m s^{-1}) by dynamic viscosity (Pa s or N s m^{-2}) and then dividing the result by the normal load per unit length of the bearing (N m^{-1}).[46] The Stribeck curve reveals the performance of the fluids in the characteristic boundary lubrication, mixed lubrication, and hydrodynamic lubrication regimes.

Fig. 7a shows that CEC has the highest COF (~0.25) in the boundary lubrication, indicating significant friction and potential for wear under boundary lubrication conditions. This contrasts with vegetable oils, which show lower COFs, suggesting better lubricity and friction reduction. Acculube LB-2000 displayed the lowest COF (~0.13) in the boundary regime, followed by safflower, sunflower, HOSO, LOSO, and canola oils. Mineral oil also shows comparable COF with vegetable oil in the boundary lubrication regime, but very poor performance in the mixed and hydrodynamic lubrication regimes. Also, in the mixed lubrication regime, CEC shows the

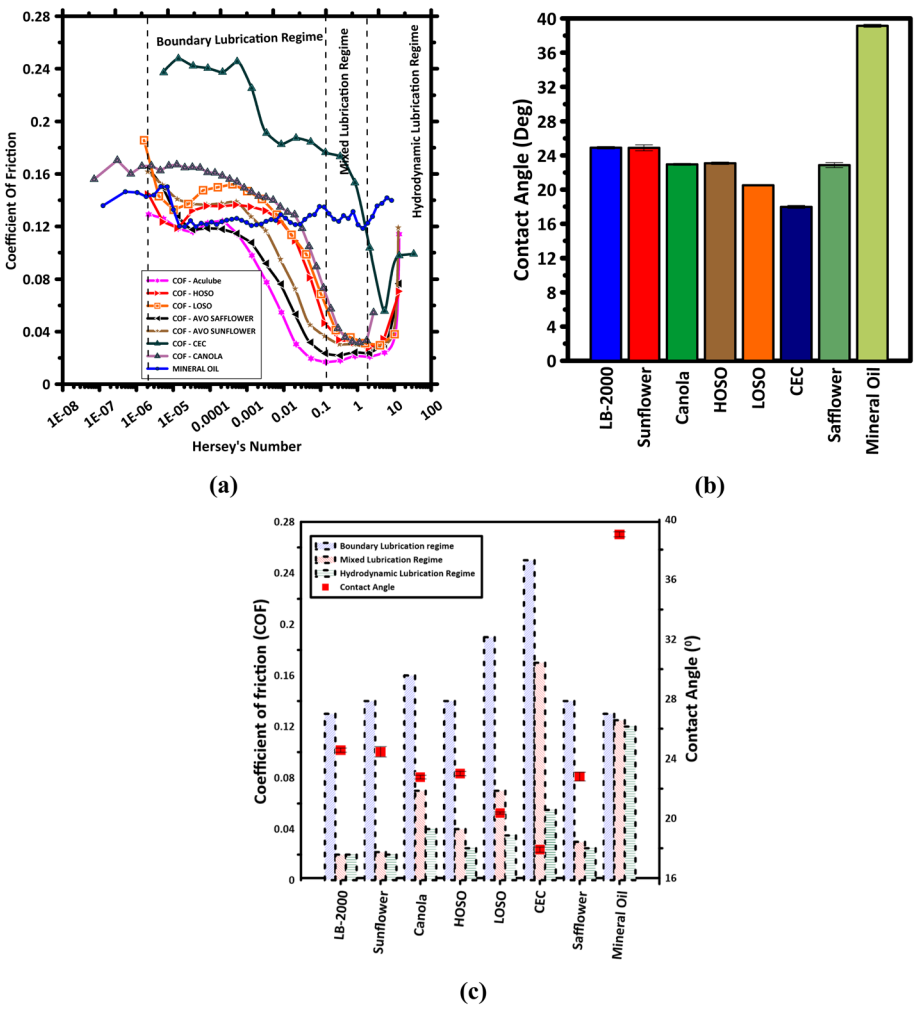

Fig. 7 Graph representing: (a) Stribeck curves, (b) contact angle, (c) the coefficient of friction at different lubrication regimes and contact angle of different vegetable oils compared to mineral oil, LB-2000 and CEC.

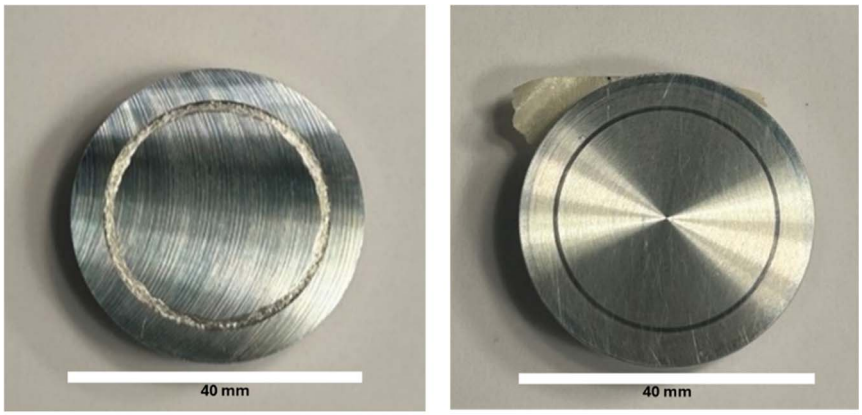

Fig. 8 Wear of the bottom aluminum plate from the tribology tests with: (a) CEC as the lubricant, and (b) HOSO vegetable oil as the lubricant.

highest COF (~0.17), indicating high friction under partial fluid film conditions. Vegetable oils-based fluids, particularly LB-2000 (~0.02) and sunflower oil (~0.022), show much lower COFs, indicating better performance due to their ability to form thicker lubricating films. Canola oil (~0.07) and LOSO (~0.07) have higher COFs but still perform better than CEC and mineral oil in the mixed lubrication regime.

In the hydrodynamic regime where a full fluid film is present, mineral oil and CEC again exhibit the highest average COF. This suggests that even in conditions favoring complete lubrication, CEC, and mineral oil are less effective compared to the vegetable oils, where LB-2000 (~0.02) and sunflower oil (~0.02) perform the best. Canola oil (0.04) has the highest COF among the vegetable oils but is still lower than that of CEC. Thus, CEC shows the higher COF across all lubrication regimes compared to the vegetable oils, indicating its poor lubrication performance (although CEC outperforms pure mineral oil in the hydrodynamic regime), while Acculube LB-2000 displayed the lowest COF across all three lubrication regimes, suggesting its superior lubricity.

Fig. 7b shows the contact angle of the fluids showing CEC with the lowest wettability and mineral oil with the highest. The vegetable oils feature a medium contact angle in the range of 20.4–24.5°, while the CEC and mineral oil show a contact angle of 17.91° and 39.02°, respectively. To better understand the relationship between film thickness and lubrication performance of the fluids, data was extracted from the three regimes and plotted in Fig. 7c in tandem with the contact angle values. As shown in Fig. 7c, CEC exhibits the lowest contact angle (17.91°), indicating the highest wettability among the lubricants. This high wettability implies that CEC spreads more readily on the surface, which might be beneficial for achieving complete surface coverage. However, higher wettability often correlates with thinner lubrication films, potentially leading to less effective separation of contacting surfaces under load. Hence the high COF of CEC in all three lubrication regimes. In contrast, vegetable oils have medium contact angles, indicating medium wettability and suggesting they will form lubrication films with a balance of flowability and surface coating ability needed to reduce friction at mixed and hydrodynamic lubrication regimes. Among the vegetable oils, the contact angles range from 20.36° (LOSO) to 24.45° (sunflower), and LB-2000 has a contact angle of 23.79°, indicating they also possess wetting properties but forms a relatively thicker film than CEC. On the other hand, mineral oil featuring a higher contact angle (39.02°) can provide film thickness to reduce friction in the boundary lubrication regime, but low flowability that hinders its performance at higher Hersey's number in the mixed and hydrodynamic lubrication regimes. From Fig. 7c it is observed that the fluid with a lower contact angle featured higher COF in the boundary layer while fluid with too high contact angle displays high COF in the mixed and hydrodynamic lubrication regimes. Thus, the balance of wettability and film thickness contributes to the vegetable oils' lubrication performance leading to a reduction in tool wear compared to CEC. Representative images of the aluminum plates used for the tribology tests are shown in Fig. 8, showing the extent of wear on the aluminum plate is much more pronounced when CEC was used (Fig. 8a) as lubricant compared to when HOSO (vegetable oils) was used (Fig. 8b).

4 Conclusions

• FTIR analysis confirmed water in CEC (3200–3600 cm^{-1}) and C–H stretching vibrations in vegetable oils (2800–3000 cm^{-1}), indicating the presence of long-chain fatty acids for lubrication. The strong absorption band at 1740–1750 cm^{-1} in vegetable oils showed ester carbonyl groups (triglycerides), while a weaker band at 1650–1660 cm^{-1} indicated unsaturated fatty acids, varying with the degree of unsaturation. In general, the IR spectra showed similar chemical compositions among vegetable oils and LB-2000.

• The vegetable oils exhibited higher viscosity, higher viscosity indices and activation energy than CEC, indicating better resistance to viscosity changes at high temperatures. However, pure mineral oil exhibited higher viscosity and viscosity index than the vegetable oils.

• TGA revealed similar oxidative-thermal stability for the vegetable oils and LB-2000, with weight loss only above 250 °C, showing potential for moderate heat applications, while stability of CEC was relatively lower. The pure mineral oil also displayed slightly lower oxidative-thermal stability compared to the vegetable oils.

• CEC's showed higher thermal conductivity and specific heat capacity due to the high-water content, indicating it's more suited for cooling lubrication at low temperatures. However, the pure mineral oil exhibited comparatively lower thermal conductivity and heat capacity than the vegetable oils and LB-2000.

• Acculube LB-2000 exhibited the best reduction of friction coefficients at all lubrication regimes. Vegetable oils like HOSO, safflower, sunflower also showed comparable low coefficient of friction, making them good candidates for high-load lubrication.

• Vegetable oils and LB-2000 had higher contact angles than CEC, suggesting thicker lubricating films for better surface protection and reduced wear in boundary lubrication conditions.

Recommendation/future work

• Nanoparticle additives: using nanoparticles like graphene, silicon carbide, or copper can improve the thermal conductivity and specific heat capacity of vegetable oils, enhancing their heat dissipation. Research should focus on finding the optimal nanoparticle type and concentration for the best cooling performance.

• Tribological testing: future studies should conduct extended tribological testing under different load and speed conditions to better assess the wear and performance of vegetable oils.

• Surfactant addition: adding surfactants can improve the contact angle, wettability, and homogeneity of vegetable oils, leading to a more stable and efficient lubricating film.

• Environmental impact: perform a thorough environmental impact assessment of vegetable oils, including biodegradability, toxicity, and lifecycle analysis, to promote their use as eco-friendly alternatives to conventional lubricants.

• Predictive models: develop predictive models to forecast the performance of vegetable oils as lubricants under various conditions, optimizing formulations for specific industrial uses.

• Economic viability: analyze the long-term cost-effectiveness of vegetable oils compared to conventional lubricants, considering nanoparticle and surfactant costs, maintenance savings, and environmental benefits.

Data availability

The data supporting this article are available in the article and its ESI.†

Conflicts of interest

There are no conflicts of interest to declare.

Acknowledgements

The U. S. National Science Foundation is acknowledged for financial support under the award number CMMI 2218786. The experiments were conducted in the Sustainable Materials Laboratory (SusMatLab) at Missouri S&T. The authors would like to thank Archer Daniels Midland Inc., and Cargill Inc., USA, for the supply of some oil samples. The results and discussions are the views of the authors.

References

1 A. Suhane, A. Rehman and H. K. Khaira, Potential of Non Edible Vegetable Oils as an Alternative Lubricants in Automotive Applications, *Int. J. Eng. Res. Ind. Appl.*, 2012, **2**(5), 1330–1335.

2 P. Nagendramma and S. Kaul, Development of Ecofriendly/Biodegradable Lubricants: An Overview, *Renewable Sustainable Energy Rev.*, 2012, **16**(1), 764–774, DOI: **10.1016/j.rser.2011.09.002**.

3 B. Sen, S. K. Yadav, G. Kumar, P. Mukhopadhyay and S. Ghosh, Performance of Eco-Benign Lubricating/Cooling Mediums in Machining of Superalloys: A Comprehensive Review from the Perspective of Triple Bottom Line Theory, *Sustainable Mater. Technol.*, 2023, **35**, e00578, DOI: **10.1016/j.susmat.2023.e00578**.

4 A. C. Okafor and T. O. Nwoguh, Comparative Evaluation of Soybean Oil–Based MQL Flow Rates and Emulsion Flood Cooling Strategy in High-Speed Face Milling of Inconel 718, *Int. J. Adv. Manuf. Technol.*, 2020, **107**(9–10), 3779–3793, DOI: **10.1007/s00170-020-05248-3**.

5 N. A. Masripan, M. A. Salim, G. Omar, M. R. Mansor, N. A. Hamid, M. I. Syakir and F. Dai, Vegetable Oil as Bio-Lubricant and Natural Additive in Lubrication: A Review, *Int. J. Nanoelectron. Mater.*, 2020, **13**, 161–176.

6 A. Hamnas and G. Unnikrishnan, Bio-Lubricants from Vegetable Oils: Characterization, Modifications, Applications and Challenges – Review, *Renewable Sustainable Energy Rev.*, 2023, **182**, 113413, DOI: **10.1016/j.rser.2023.113413**.

7 B. Sen, M. Mia, G. M. Krolczyk, U. K. Mandal and S. P. Mondal, Eco-Friendly Cutting Fluids in Minimum Quantity Lubrication Assisted Machining: A Review on the Perception of Sustainable Manufacturing, *Int. J. Precis. Eng. Manuf. - Green Technol.*, 2021, **8**(1), 249–280, DOI: **10.1007/s40684-019-00158-6**.

8 S. P. Darminesh, N. A. C. Sidik, G. Najafi, R. Mamat, T. L. Ken and Y. Asako, Recent Development on Biodegradable Nanolubricant: A Review, *Int. Commun. Heat Mass Transfer*, 2017, **86**, 159–165, DOI: **10.1016/j.icheatmasstransfer.2017.05.022**.

9 S. Debnath, M. M. Reddy and Q. S. Yi, Environmental Friendly Cutting Fluids and Cooling Techniques in

Machining: A Review, *J. Cleaner Prod.*, 2014, **83**, 33–47, DOI: 10.1016/j.jclepro.2014.07.071.
10 A. C. Okafor and T. O. Nwoguh, Comparative Evaluation of Soybean Oil–Based MQL Flow Rates and Emulsion Flood Cooling Strategy in High-Speed Face Milling of Inconel 718, *Int. J. Adv. Manuf. Technol.*, 2020, **107**(9), 3779–3793, DOI: 10.1007/s00170-020-05248-3.
11 I. Stanciu, Viscosity Index for Oil Used as Biodegradable Lubricant, *Indian J. Sci. Technol.*, 2020, **13**(3), 352–359, DOI: 10.17485/ijst/2020/v13i03/147759.
12 J. D. Leao, V. Bouillon, L. Muntada, C. Johnson, P. Wilson, O. Vergnes, C. Dano, A. Igartua and G. Mendoza, New Formulations of Sunflower Based Bio-Lubricants with High Oleic Acid Content – VOSOLUB Project, *OCL:Oilseeds Fats, Crops Lipids*, 2016, **23**(5), D509, DOI: 10.1051/ocl/2016033.
13 K. N. Anand and J. Mathew, Evaluation of Size Effect and Improvement in Surface Characteristics Using Sunflower Oil-Based MQL for Sustainable Micro-Endmilling of Inconel 718, *J. Braz. Soc. Mech. Sci. Eng.*, 2020, **42**(4), 156, DOI: 10.1007/s40430-020-2239-0.
14 N. J. Fox, B. Tyrer and G. W. Stachowiak, Boundary Lubrication Performance of Free Fatty Acids in Sunflower Oil, *Tribol. Lett.*, 2004, **16**(4), 275–281, DOI: 10.1023/B:TRIL.0000015203.08570.82.
15 L. Ugolini, R. Matteo, L. Lazzeri, L. Malaguti, L. Folegatti, P. Bondioli, D. Pochi, R. Grilli, L. Fornaciari, S. Benigni and R. Fanigliulo, Technical Performance and Chemical–Physical Property Assessment of Safflower Oil Tested in an Experimental Hydraulic Test Rig, *Lubricants*, 2023, **11**(2), 39, DOI: 10.3390/lubricants11020039.
16 S. Nogales-Delgado, J. M. Encinar and Á. González Cortés, High Oleic Safflower Oil as a Feedstock for Stable Biodiesel and Biolubricant Production, *Ind. Crops Prod.*, 2021, **170**, 113701, DOI: 10.1016/j.indcrop.2021.113701.
17 A. S. Araújo Junior, W. F. Sales, R. B. da Silva, E. S. Costa and Á. Rocha Machado, Lubri-Cooling and Tribological Behavior of Vegetable Oils during Milling of AISI 1045 Steel Focusing on Sustainable Manufacturing, *J. Cleaner Prod.*, 2017, **156**, 635–647, DOI: 10.1016/j.jclepro.2017.04.061.
18 Y. Zhang, H. N. Li, C. Li, C. Huang, H. M. Ali, X. Xu, C. Mao, W. Ding, X. Cui, M. Yang, T. Yu, M. Jamil, M. K. Gupta, D. Jia and Z. Said, Nano-Enhanced Biolubricant in Sustainable Manufacturing: From Processability to Mechanisms, *Friction*, 2022, **10**(6), 803–841, DOI: 10.1007/s40544-021-0536-y.
19 N. Talib and E. A. Rahim, The Effect of Tribology Behavior on Machining Performances When Using Bio-Based Lubricant as a Sustainable Metalworking Fluid, *Procedia CIRP*, 2016, **40**, 504–508, DOI: 10.1016/j.procir.2016.01.116.
20 R. Kozdrach, The Comparative Analysis of Ecological Lubricants, *Tribologia*, 2022, **4**, 17–22, DOI: 10.24874/ti.941.08.20.11.
21 R. Kozdrach and B. Skowronski, The Application of Chitosan as a Modifier for Lubricating Greases Based on Vegetable Oil, *Tribol. Ind.*, 2019, **41**(2), 212–219, DOI: 10.24874/ti.2019.41.02.07.
22 R. Kozdrach and J. Skowroński, The Application of Polyvinylpyrrolidone as a Modifier of Tribological Properties of Lubricating Greases Based on Linseed Oil, *J. Tribol.*, 2018, **140**, 061801, DOI: 10.1115/1.4040054.
23 R. Kozdrach, The Tribological Properties of Lubricating Greases Produced on Vegetable Base and Modified of Polytetrafluoroethylene, *Tribologia*, 2020, **37**(1–2), 4–14, DOI: 10.30678/fjt.84884.
24 T. O. Nwoguh, A. C. Okafor and H. A. Onyishi, Enhancement of Viscosity and Thermal Conductivity of Soybean Vegetable Oil Using Nanoparticles to Form Nanofluids for Minimum Quantity Lubrication Machining of Difficult-to-Cut Metals, *Int. J. Adv. Manuf. Technol.*, 2021, **113**(11), 3377–3388, DOI: 10.1007/s00170-021-06812-1.
25 A. C. Okafor, T. K. Abor, S. E. Valiev, I. E. Ekengwu, A. Saka and M. U. Okoronkwo, Thermal Conductivity Characterization of High Oleic Vegetable Oils Based Hybrid-Nanofluids Formulated Using GnP, TiO2, MoS2, Al2O3 Nanoparticles for MQL Machining, *Int. J. Thermophys.*, 2024, **45**, 169, DOI: 10.1007/s10765-024-03472-7.
26 R. Kozdrach, The Tribological and Rheological Properties of Vegetable Lubricating Grease Modified of TiO2 Nanoparticles, *Tribol. Ind.*, 2024, **46**(1), 80–96, DOI: 10.24874/ti.1523.07.23.09.
27 L. Honary, *Performance of Selected Vegetable Oils in ASTM Hydraulic Tests*, SAE International, 1995, DOI: 10.4271/952075.
28 J. L. Glancey, S. Knowlton and E. R. Benson, Development of a High Oleic Soybean Oil-Based Hydraulic Fluid, *SAE Trans.*, 1998, **107**, 266–269.
29 M. U. Okoronkwo, G. Falzone, A. Wada, W. Franke, N. Neithalath and G. Sant, Rheology-Based Protocol to Establish Admixture Compatibility in Dense Cementitious Suspensions, *J. Mater. Civ. Eng.*, 2018, **30**(7), 04018122, DOI: 10.1061/(ASCE)MT.1943-5533.0002277.
30 S. K. Mondal, A. Welz, C. Clinton, K. Khayat, A. Kumar and M. U. Okoronkwo, Quantifying the Workability of Calcium Sulfoaluminate Cement Paste Using Time-Dependent Rheology, *Materials*, 2022, **15**(16), 5775, DOI: 10.3390/ma15165775.
31 G. K. Batchelor, *An Introduction to Fluid Dynamics*, Cambridge University Press, 1967.
32 E. Bingham, An Investigation of the Laws of Plastic Flow, *Bull. Bur. Stand.*, 1916, **13**(2), 309–354.
33 R. P. Chhabra and J. F. Richardson, *Non-Newtonian Flow and Applied Rheology: Engineering Applications*, Elsevier, New York, 2nd edn, 2008.
34 L. L. Schramm, *Emulsions, Foams, and Suspensions: Fundamentals and Applications*, John Wiley & Sons, Germany, 2006.
35 T. Mezger, *The Rheology Handbook: for Users of Rotational and Oscillatory Rheometers*, Vincentz Network: European Coatings, Hanover, 2020.
36 J. Kim, D. N. Kim, S. H. Lee, S.-H. Yoo and S. Lee, Correlation of Fatty Acid Composition of Vegetable Oils with Rheological

Behaviour and Oil Uptake, *Food Chem.*, 2010, **118**(2), 398–402, DOI: 10.1016/j.foodchem.2009.05.011.

37 G. Czechowski and J. Jadżyn, The Viscous Properties of Diols. I. The Homologous Series of 1,2- and 1,n-Alkanediols, *Z. Naturforsch. A*, 2003, **58**(5–6), 317–320, DOI: 10.1515/zna-2003-5-612.

38 ASTM D2270 Standard, *Practice for Calculating Viscosity Index from Kinematic Viscosity at 40 and 100C*, ASTM International, 2016, DOI: 10.1520/D2270-10R16.

39 N. Saadatkhah, A. Carillo Garcia, S. Ackermann, P. Leclerc, M. Latifi, S. Samih, G. S. Patience and J. Chaouki, Experimental Methods in Chemical Engineering: Thermogravimetric Analysis—TGA, *Can. J. Chem. Eng.*, 2020, **98**(1), 34–43, DOI: 10.1002/cjce.23673.

40 B. D. Lawrence, S. Wharram, J. A. Kluge, G. G. Leisk, F. G. Omenetto, M. I. Rosenblatt and D. L. Kaplan, Effect of Hydration on Silk Film Material Properties: Effect of Hydration on Silk Film Material Properties, *Macromol. Biosci.*, 2010, **10**(4), 393–403, DOI: 10.1002/mabi.200900294.

41 B. L. Taylor and T. B. Mills, Using a Three-Ball-on-Plate Configuration for Soft Tribology Applications, *J. Food Eng.*, 2020, **274**, 109838, DOI: 10.1016/j.jfoodeng.2019.109838.

42 TA Instruments–Waters LLC, Tribo-Rheometry Test Geometries, http://www.ifug.ugto.mx/~labblanda/manuales/Content/ARESTopics/ARES_Tests/TribologyTestFixtures.htm (accessed 2024-11-18).

43 ASTM Standard G99. Standard Test Method for Wear and Friction Testing with a Pin-on-Disk or Ball-on-Disk Apparatus, 2023, https://compass.astm.org/document/?contentCode=ASTM%7CG0099-23%7Cen-US&proxycl=https%3A%2F%2Fsecure.astm.org&fromLogin=true (accessed 2024-11-18).

44 *Tribology for Scientists and Engineers: from Basics to Advanced Concepts*, ed. Menezes, P. L., Nosonovsky, M., Ingole, S. P., Kailas, S. V. and Lovell, M. R., Springer, New York, NY, 2013, DOI: 10.1007/978-1-4614-1945-7.

45 L. Wang, J. Cai, J. Zhou and J. Duszczyk, Characteristics of the Friction Between Aluminium and Steel at Elevated Temperatures During Ball-on-Disc Tests, *Tribol. Lett.*, 2009, **36**(2), 183–190, DOI: 10.1007/s11249-009-9475-x.

46 Y. Wang and Q. J. Wang, Stribeck Curves, in *Encyclopedia of Tribology*, ed. Wang, Q. J. and Chung, Y.-W., Springer, Boston, MA, US, 2013, pp. 3365–3370, DOI: 10.1007/978-0-387-92897-5_148.

47 H. J. Bakker and J. L. Skinner, Vibrational Spectroscopy as a Probe of Structure and Dynamics in Liquid Water, *Chem. Rev.*, 2010, **110**(3), 1498–1517, DOI: 10.1021/cr9001879.

48 J. Lindner, P. Vöhringer, M. S. Pshenichnikov, D. Cringus, D. A. Wiersma and M. Mostovoy, Vibrational Relaxation of Pure Liquid Water, *Chem. Phys. Lett.*, 2006, **421**(4), 329–333, DOI: 10.1016/j.cplett.2006.01.081.

49 B. Louise Mojet, S. Dalgaard Ebbesen and L. Lefferts, Light at the Interface: The Potential of Attenuated Total Reflection Infrared Spectroscopy for Understanding Heterogeneous Catalysis in Water, *Chem. Soc. Rev.*, 2010, **39**(12), 4643–4655, DOI: 10.1039/C0CS00014K.

50 D. Eisenberg and W. Kauzmann, *The Structure and Properties of Water*, Oxford University Press, 1969.

51 M. P. Bernstein, S. A. Sandford and L. J. Allamandola, The Infrared Spectra of Nitriles and Related Compounds Frozen in Ar and H2O, *Astrophys. J.*, 1997, **476**(2), 932, DOI: 10.1086/303651.

52 S. L. Crawley, J. A. Kocsis, M. D. Gieselman and P. E. Mosier, Lubricating Composition Containing a Nitrile Compound, *US Pat.*, US20120309655A1, December 6, 2012, https://patents.google.com/patent/US20120309655A1/en, accessed 2024-09-15.

53 D. I. Hoke, Lubricants and Functional Fluids Containing Polyfunctional Nitriles, *US Pat.*, US4058469A, November 15, 1977, https://patents.google.com/patent/US4058469A/en (accessed 2024-09-15).

54 A. L. Smith, *The Coblentz Society Desk Book of Infrared Spectra*, ed. Carver, C. D., The Coblentz Society, Kirkwood, MO, 2nd edn, 1982.

55 H. Kalathiripi and S. Karmakar, Analysis of Transformer Oil Degradation Due to Thermal Stress Using Optical Spectroscopic Techniques, *Int. Trans. Electr. Energy Syst.*, 2017, **27**(9), e2346, DOI: 10.1002/etep.2346.

56 Wear of Metal by Rubber, Tribology of Elastomers, in *Tribology and Interface Engineering Series*, ed. Zhang, S.-W., Elsevier, 2004, vol. 47, pp. 227–246, DOI: 10.1016/S0167-8922(04)80011-7.

57 L. da Silva Dutra, M. N. de Souza and J. C. Pinto, Preparation of Polymer Microparticles Through Non-Aqueous Suspension Polycondensations: Part IV—Effect of the Continuous Phase on the Characteristics of Final Poly(Butylene Succinate) Particles, *J. Polym. Environ.*, 2021, **29**(1), 219–229, DOI: 10.1007/s10924-020-01869-7.

58 J. Xu, M. Chen, C. Zhang and X. Wu, First-Principles Study of the Infrared Spectrum in Liquid Water from a Systematically Improved Description of H-Bond Network, *Phys. Rev. B*, 2019, **99**(20), 205123, DOI: 10.1103/PhysRevB.99.205123.

59 M. D. Guillén and N. Cabo, Characterization of Edible Oils and Lard by Fourier Transform Infrared Spectroscopy. Relationships between Composition and Frequency of Concrete Bands in the Fingerprint Region, *J. Am. Oil Chem. Soc.*, 1997, **74**(10), 1281–1286, DOI: 10.1007/s11746-997-0058-4.

60 M. D. Guillén and N. Cabo, Fourier Transform Infrared Spectra Data versus Peroxide and Anisidine Values to Determine Oxidative Stability of Edible Oils, *Food Chem.*, 2002, **77**(4), 503–510, DOI: 10.1016/S0308-8146(01)00371-5.

61 H. Nosal, K. Moser, M. Warzała, A. Holzer, D. Stańczyk and E. Sabura, Selected Fatty Acids Esters as Potential PHB-V Bioplasticizers: Effect on Mechanical Properties of the Polymer, *J. Polym. Environ.*, 2021, **29**(1), 38–53, DOI: 10.1007/s10924-020-01841-5.

62 H. F. George and F. Qureshi, Newton's Law of Viscosity, Newtonian and Non-Newtonian Fluids, in *Encyclopedia of Tribology*, ed. Wang, Q. J. and Chung, Y.-W., Springer, Boston, MA, US, 2013, pp. 2416–2420, DOI: 10.1007/978-0-387-92897-5_143.

63 S. Li, L. Jiang and X. J. Zhang, Investigation on the Influence of Dispersion Mass Transfer on the Thermal Characteristics of Phase Change Emulsion, *Sol. Energy Mater. Sol. Cells*, 2022, **236**, 111552, DOI: **10.1016/j.solmat.2021.111552**.

64 L. M. Diamante and T. Lan, Absolute Viscosities of Vegetable Oils at Different Temperatures and Shear Rate Range of 64.5 to 4835 s^{-1}, *J. Food Process.*, 2014, **2014**, 1–6, DOI: **10.1155/2014/234583**.

65 C. Tangsathitkulchai, Y. Sittichaitaweekul and M. Tangsathitkulchai, Temperature Effect on the Viscosities of Palm Oil and Coconut Oil Blended with Diesel Oil, *J. Am. Oil Chem. Soc.*, 2004, **81**(4), 401–405, DOI: **10.1007/s11746-004-0913-8**.

66 M. Peleg, M. D. Normand and M. G. Corradini, The Arrhenius Equation Revisited, *Crit. Rev. Food Sci. Nutr.*, 2012, **52**(9), 830–851, DOI: **10.1080/10408398.2012.667460**.

67 Y. N. Starodubtsev, V. S. Tsepelev, V. V. Konashkov and N. P. Tsepeleva, The Activation Energy of Viscous Flow and Liquid–Liquid Structure Transition in Co-B Alloys, *Metals*, 2023, **13**(12), 1954, DOI: **10.3390/met13121954**.

68 H. Eyring, Viscosity, Plasticity, and Diffusion as Examples of Absolute Reaction Rates, *J. Chem. Phys.*, 1936, **4**(4), 283–291, DOI: **10.1063/1.1749836**.

69 J. C. Dyre, N. B. Olsen and T. Christensen, Local Elastic Expansion Model for Viscous-Flow Activation Energies of Glass-Forming Molecular Liquids, *Phys. Rev. B*, 1996, **53**(5), 2171–2174, DOI: **10.1103/PhysRevB.53.2171**.

70 O. O. Fasina, H. Hallman, M. Craig-Schmidt and C. Clements, Predicting Temperature-Dependence Viscosity of Vegetable Oils from Fatty Acid Composition, *J. Am. Oil Chem. Soc.*, 2006, **83**(10), 899–903, DOI: **10.1007/s11746-006-5044-8**.

71 A.-A. A. Abdel-Azim and R. M. Abdel-Aziem, Polymeric Additives for Improving the Flow Properties and Viscosity Index of Lubricating Oils, *J. Polym. Res.*, 2001, **8**(2), 111–118, DOI: **10.1007/s10965-006-0140-x**.

72 A. M. Nassar, Synthesis and Evaluation of Viscosity Index Improvers and Pour Point Depressant for Lube Oil, *Pet. Sci. Technol.*, 2008, **26**(5), 523–531, DOI: **10.1080/10916460600809519**.

73 J. D. Moore, S. T. Cui, P. T. Cummings and H. D. Cochran, Lubricant Characterization by Molecular Simulation, *AIChE J.*, 1997, **43**(12), 3260–3263, DOI: **10.1002/aic.690431215**.

74 A. Kabuya and J. L. Bozet, Comparative Analysis of the Lubricating Power between a Pure Mineral Oil and Biodegradable Oils of the Same Mean Iso Grade, in *Tribology Series Lubricants and Lubrication*, ed. Dowson, D., Taylor, C. M., Childs, T. H. C. and Dalmaz, G., Elsevier, 1995, vol. 30, pp. 25–30, DOI: **10.1016/S0167-8922(08)70613-8**.

75 N. W. M. Zulkifli, M. A. Kalam, H. H. Masjuki, M. Shahabuddin and R. Yunus, Wear Prevention Characteristics of a Palm Oil-Based TMP (Trimethylolpropane) Ester as an Engine Lubricant, *Energy*, 2013, **54**, 167–173, DOI: **10.1016/j.energy.2013.01.038**.

76 B. K. Sharma, A. Adhvaryu and S. Z. Erhan, Friction and Wear Behavior of Thioether Hydroxy Vegetable Oil, *Tribol. Int.*, 2009, **42**(2), 353–358, DOI: **10.1016/j.triboint.2008.07.004**.

77 S. A. Smith, R. E. King and D. B. Min, Oxidative and Thermal Stabilities of Genetically Modified High Oleic Sunflower Oil, *Food Chem.*, 2007, **102**(4), 1208–1213, DOI: **10.1016/j.foodchem.2006.06.058**.

78 S. M. Abdulkarim, K. Long, O. M. Lai, S. K. S. Muhammad and H. M. Ghazali, Frying Quality and Stability of High-Oleic Moringa Oleifera Seed Oil in Comparison with Other Vegetable Oils, *Food Chem.*, 2007, **105**(4), 1382–1389, DOI: **10.1016/j.foodchem.2007.05.013**.

79 R. Romano, N. Manzo, L. Le Grottaglie, A. Giordano, A. Romano and P. Masi, Comparison of the Frying Performance of High Oleic Oils Subjected to Discontinuous and Prolonged Thermal Treatment, *J. Am. Oil Chem. Soc.*, 2013, **90**(7), 965–975, DOI: **10.1007/s11746-013-2238-8**.

80 L.-P. Zhou, B.-X. Wang, X.-F. Peng, X.-Z. Du and Y.-P. Yang, On the Specific Heat Capacity of CuO Nanofluid, *Adv. Mech. Eng.*, 2010, **2**, 172085, DOI: **10.1155/2010/172085**.

81 B. Bustami, M. M. Rahman, M. J. Shazida, M. Islam, M. H. Rohan, S. Hossain, A. S. M. Nur and H. Younes, Recent Progress in Electrically Conductive and Thermally Conductive Lubricants: A Critical Review, *Lubricants*, 2023, **11**(8), 331, DOI: **10.3390/lubricants11080331**.